Hydrodynamics of Oscillating Disks in Viscous Fluids: Density and Viscosity of Normal Fluid in Pure He^4 from 1.2°K to the Lambda Point*

J. G. Dash and R. Dean Taylor
Los Alamos Scientific Laboratory of the University of California, Los Alamos, New Mexico
(Received April 23, 1956; revised manuscript received September 20, 1956)

A new study has been made of the viscous component in liquid He II, using the experimental method of Andronikashvili. The hydrodynamic equations for disks oscillating in a viscous medium have been derived from first principles in a form amenable to experimental test of the necessary approximations. Associated studies with several ordinary liquids have yielded an empirical constant for the liquid dragged by the disk corner. The final semi-empirical equations of motion appear to provide a significantly better approximation than those previously published. The new formulas have been applied to a combined study of density and viscosity of pure He^4 liquid from 1.2°K to the lambda point, 2.1735°K. Refinements in experimental technique include larger oscillating systems, improved temperature regulation and measurement, and precision chronometry. The theoretical roton temperature dependence of Landau and of Feynman provides a good description of the density between 1.2° and 2.0°K. The empirical value of the roton excitation energy is found to be $\Delta/k=10.60$°K. Detailed investigation in the region of the lambda point shows an accelerated rise in the normal fluid density above 2.0°K; the temperature derivative of density tends toward infinity at T_λ. Our data confirm the measurements made earlier by Andronikashvili over the entire temperature range. At temperatures below 1.5°K the torsion pendulum results lie significantly lower than those derived from second sound and specific heat data. Viscosities of the normal fluid are in substantial agreement with the earlier results of Andronikashvili and with the viscometer values of Heikkila and Hallett down to 1.5°K. Discrepancies between the oscillating disk and viscometer data below 1.5°K have not been resolved. The temperature dependence of the viscosity near the lambda point indicates that T_λ is a point of strong singularity for both viscosity and normal fluid density.

I. INTRODUCTION

In terms of present theories of He II, a complete description of the hydrodynamics of the liquid requires the specification of the normal fluid density ρ_n, the normal fluid viscosity η, the critical velocity v_c, and supercritical resistance to the flow of the superfluid.[1] These properties are functions of the temperature and of He^3 isotope concentration; critical velocity phenomena appear to depend also upon the experimental liquid dimensions. This complex of flow properties may be studied by means of the torsion pendulum, which has been applied to the measurement of viscosity since Coulomb's inception of the method in 1784. With some modifications, it is particularly applicable to the study of liquid helium and has been so applied by several investigators.[2–7] It is the technique adopted by the authors in the research reported here.

In spite of considerable interest in the problem, it has not been possible to obtain an exact solution for the torsional oscillations of a right circular cylinder in a viscous fluid. Nevertheless, this geometry is an experimentally desirable one and has been employed in the present work. Since previous publications are in disagreement in the analysis of the problem, we have undertaken a new theoretical study of the hydrodynamics. Associated experiments with several Newtonian fluids indicate that the new analysis provides an improved approximation.

The formulas derived here have been applied to a systematic investigation of He II to obtain ρ_n, η, v_c, and supercritical resistance as functions of the temperature, He^3 concentration, and liquid dimensions. The present paper reports the study of ρ_n and η in pure He^4 in the temperature range 1.2°K to the lambda point.

II. THEORY OF OSCILLATING DISKS

Statement of the Problem

A right circular cylinder of radius a, height d, and moment of inertia I is suspended from a fiber of torsion constant L and oscillates slowly about its symmetry axis according to

$$I(d\dot{\theta}/dt)+K\dot{\theta}+L\theta=0, \quad (1)$$

where θ is the angular displacement of the disk from its equilibrium position, and $\dot{\theta}\equiv d\theta/dt$. Terms in θ^2 and $\dot{\theta}^2$, and higher orders are neglected. The implicit solution of the differential equation represents damped harmonic motion,

$$\theta=\theta_0 \exp\alpha t; \quad \alpha=(2\pi/\tau)(i-\delta), \quad (2)$$

where $i=\sqrt{-1}$, τ is the period of oscillation, and $2\pi\delta$ is the logarithmic decrement of amplitude. The relationship between the observables δ, τ, and the complex damping coefficient K is obtained by substituting Eq.

* A preliminary report on this research was presented at the National Science Foundation Conference on Low Temperature Physics and Chemistry, December 28–30, 1955, at Louisiana State University.

[1] For recent reviews of the liquid helium problem, see J. G. Daunt and R. S. Smith, Revs. Modern Phys. **26**, 172 (1954), and *Progress in Low Temperature Physics*, edited by C. J. Gorter (Interscience Publishers, Inc., New York, 1955).

[2] W. H. Keesom and G. E. MacWood, Physica **5**, 737 (1938).

[3] E. L. Andronikashvili, J. Phys. (U.S.S.R.) **10**, 201 (1946).

[4] E. L. Andronikashvili, J. Exptl. Theoret. Phys. (U.S.S.R.) **18**, 424 (1948).

[5] E. L. Andronikashvili, J. Exptl. Theoret. Phys. (U.S.S.R.) **18**, 429 (1948).

[6] De Troyer, van Itterbeek, and van den Berg, Physica **17**, 50 (1951).

[7] A. C. Hollis Hallett, Proc. Roy. Soc. (London) **A210**, 404 (1951).

(2) in Eq. (1):

$$\begin{aligned}\mathrm{Re}\,K&=2\pi I\delta[(\tau^2/\tau_0^2)+1]\tau^{-1},\\ \mathrm{Im}\,K&=2\pi I[(\tau^2/\tau_0^2)-1]\tau^{-1},\end{aligned}\tag{3}$$

where we have substituted $L=4\pi^2 I/\tau_0^2$, τ_0 being the natural period of the pendulum in vacuum. Terms in δ^2 are neglected.

The medium considered is a fluid whose viscosity η is well behaved and is not subject to slip, i.e., for a relative velocity component v_y parallel to a solid boundary at $x=0$,

$$f_y=-\eta(dv_y/dx)_{x=0},\quad (v_y)_{x=0}=0,\tag{4}$$

where f_y is the tangential force per unit area. In the present application, the medium is subjected to purely shearing stresses. Since a fluid is characterized by the complete absence of rigidity for slow motions, the shear distortions do not introduce fluctuations in the density, whether or not the fluid is considered to be "compressible" in the usual sense. According to the equation of continuity of mass, the constancy of ρ implies that $\nabla\cdot\mathbf{v}=0$. We assume laminar flow and zero pressure gradient along the streamlines. The velocity field is described by the simplified Navier-Stokes equation,

$$\rho(d\mathbf{v}/dt)-\eta\nabla^2\mathbf{v}=0.\tag{5}$$

We assume that the fluid rotates about the symmetry axis of the disk with no radial or axial velocity components. Defining $\psi(r,z,t)$ as the angular displacement field, we have $v=r\dot{\psi}$, where $\dot{\psi}=\partial\psi/\partial t$. Equation (5) reduces to the scalar equation in cylindrical coordinates[8];

$$\frac{\partial^2\dot{\psi}}{\partial r^2}+\frac{3}{r}\frac{\partial\dot{\psi}}{\partial r}+\frac{\partial^2\dot{\psi}}{\partial z^2}-\frac{\rho}{\eta}\frac{\partial\dot{\psi}}{\partial t}=0.\tag{6}$$

If we assume that ψ is of the form $\psi(r,z,t)=\varphi(r,z)T(t)$, then Eq. (6) yields

$$T(t)=\exp(\alpha t+\gamma)=\text{const}\,\exp(\alpha t)\tag{7}$$

and

$$\frac{\partial^2\varphi}{\partial r^2}+\frac{3}{r}\frac{\partial\varphi}{\partial r}+\frac{\partial^2\varphi}{\partial z^2}-p^2\varphi=0,\tag{8}$$

where $p^2=\rho\alpha/\eta$.

Independent Radial and Axial Solutions

In this approximation, motion of the fluid is treated as if induced by the plane faces and the cylindrical edge acting independently. If we assume, therefore, that $\varphi(r,z)=R(r)+Z(z)$, Eq. (8) is reduced to two one-dimensional equations,

$$\text{Edge:}\quad \frac{d^2R}{dr^2}+\frac{3}{r}\frac{dR}{dr}-p^2R=0,\tag{9a}$$

$$\text{Faces:}\quad \frac{d^2Z}{dz^2}-p^2Z=0.\tag{9b}$$

The general solutions are

$$\begin{aligned}&Z=e^{\pm pz},\quad R=H_1^{(1)}(ipr)/r,\quad H_1^{(2)}(ipr)/r,\\ &p=[(1-\delta)^{\frac{1}{2}}+i(1+\delta)^{\frac{1}{2}}]/\lambda;\quad \lambda=(\tau\eta/\pi\rho)^{\frac{1}{2}},\end{aligned}\tag{10}$$

where $H^{(1)}$, $H^{(2)}$ are Hankel functions of the first and second kind. λ is the "boundary layer" thickness or "penetration depth" of viscous shear waves, the distance in which the disturbance in the fluid falls off to $1/e$ (only approximately in the case of the radial solution) of its value at the solid boundary.

Case A. Infinite medium

Applying the boundary conditions

$$\begin{aligned}&R=\theta_0 \text{ at } r=a;\quad R=0 \text{ at } r=\infty,\\ &Z=\theta_0 \text{ at } z=\pm d/2;\quad Z=0 \text{ at } z=\pm\infty,\end{aligned}$$

we obtain

$$R=\theta_0[aH_1^{(1)}(ipr)/rH_1^{(1)}(ipa)],\tag{11}$$

$$Z_{z>0}=\theta_0 e^{p(\frac{1}{2}d-z)};\quad Z_{z<0}=\theta_0 e^{p(\frac{1}{2}d+z)}.\tag{12}$$

The torque exerted by the independent liquid motions against the two faces and the edge of the disk is, according to Eqs. (4), (7), and (12),

$$\begin{aligned}f=(K\dot{\theta})_{\text{liquid}}&=-2\pi a^3 d\eta\dot{T}(t)\left(\frac{\partial R}{\partial r}\right)_a\\ &\quad-4\pi\dot{T}(t)\int_0^a r^3\left(\frac{\partial Z}{\partial z}\right)_{d/2}dr\\ &=-2\pi a^3 d\eta\alpha e^{\alpha t}\left(\frac{\partial R}{\partial r}\right)_a+\pi a^4\eta p\dot{\theta}.\end{aligned}\tag{13}$$

In order to obtain a convenient analytic form for the radial term, the Hankel function is expressed as the asymptotic expansion for large argument[9];

$$H_1^{(1)}(ipr)=-\left(\frac{2}{\pi pr}\right)^{\frac{1}{2}}e^{-pr}\left[1+\frac{3}{8pr}-\frac{15}{128p^2r^2}+\cdots\right].\tag{14}$$

Differentiating the radial solution Eq. (11), we obtain the radial displacement gradient at the edge of the disk,

$$\left(\frac{\partial R}{\partial r}\right)_a=-\left[p+\frac{3}{2a}+\sim\frac{3}{8pa^2}\cdots\right]\theta_0.\tag{15}$$

[8] M. Brillouin, *Leçons sur la Viscosité des Liquides et des Gaz* (Gauthier-Villars, Paris, 1907), Vol. I, p. 88. This treatise contains an excellent critical review of early experimental and theoretical researches on viscous laminar flow.

[9] E. Jahnke and F. Emde, *Tables of Functions* (Dover Publications, New York, 1945), fourth edition, pp. 137–8.

In almost all liquid helium work on torsion pendulums, $|p| \geq 5/a$, $a \sim 1$. The neglect of all terms in the expansion beyond the first two will therefore introduce an error in $(\partial R/\partial r)_a$ of the order of 8% or less. Furthermore, the drag on the edges of the relatively thin disks actually studied is usually less than 25% of the total. We will accordingly neglect the contributions due to higher order terms in the expansion with a consequent error no greater than 2%. With this simplification the liquid torque Eq. (13) becomes

$$(K\dot{\theta})_{\text{liquid}} = \pi a^4 \eta p \left[1 + \frac{2d}{a} + \frac{3d}{pa^2}\right]\dot{\theta}. \tag{16}$$

Substituting for p, we obtain the real and imaginary torques due to the liquid, which are equated to the corresponding components in Eq. (3) to yield

$$\text{Re}\left[(\eta\rho)^{\frac{1}{2}}\right] = \frac{2I\delta(\tau^2/\tau_0^2+1)}{a^4[\pi\tau(1-\delta)]^{\frac{1}{2}}(1+2d/a+3\lambda d/a^2)}, \tag{17a}$$

$$\text{Im}\left[(\eta\rho)^{\frac{1}{2}}\right] = \frac{2I(\tau^2/\tau_0^2-1)}{a^4[\pi\tau(1+\delta)]^{\frac{1}{2}}(1+2d/a)}. \tag{17b}$$

Case B. Bounded medium

The disk is assumed to be centered in a cylindrical volume of fluid of radius b and height h. When we apply the proper boundary conditions, the face and edge solutions for the liquid motion are

$$Z_{z>0} = \theta_0\left[\frac{e^{-pz} - e^{p(z-h)}}{e^{-pd/2} - e^{p(d/2-h)}}\right], \tag{18a}$$

$$R = \frac{a\theta_0}{r}\left[\frac{H_{2b}H_{1r} - H_{1b}H_{2r}}{H_{1a}H_{2b} - H_{1b}H_{2a}}\right], \tag{18b}$$

where

$$H_{1r} = H_1^{(1)}(ipr), \quad H_{2r} = H_1^{(2)}(ipr), \quad \text{etc.}$$

We treat separately the two limiting cases of an "almost infinite" volume which has as its asymptotic solution Case A, and the strongly confined condition which approaches the case of steady rotation of the disk.

Case B-1. "Almost infinite" medium.—The liquid torque, and hence the computed quantity $(\rho\eta)^{-\frac{1}{2}}$, is proportional to the velocity gradient. We may then derive a criterion for the error in $(\rho\eta)^{-\frac{1}{2}}$ by comparing the gradients $(\partial R/\partial r)_{\text{bounded}}$, $(\partial Z/\partial z)_{\text{bounded}}$ from Eq. (18) with the gradients $(\partial R/\partial r)_\infty$, $(\partial Z/\partial z)_\infty$ given by the infinite medium. Approximating the Hankel functions by the first terms of their asymptotic expansions, we obtain similar expressions for the approximate percentage errors in the gradients at the faces and the edge:

$$\left|\left\{\left(\frac{\partial R}{\partial r}\right)_{\text{bounded}} - \left(\frac{\partial R}{\partial r}\right)_\infty\right\}\left(\frac{\partial R}{\partial r}\right)_\infty^{-1}\right|_{r=a} = \Delta_r = 2e^{-2|p(b-a)|}, \tag{19a}$$

$$\left|\left\{\left(\frac{\partial Z}{\partial z}\right)_{\text{bounded}} - \left(\frac{\partial Z}{\partial z}\right)_\infty\right\}\left(\frac{\partial Z}{\partial z}\right)_\infty^{-1}\right|_{z=d/2} = \Delta_z = 2e^{-2|p(h-d)|}. \tag{19b}$$

Thus it is necessary to provide a ratio $(b-a)/\lambda > 4$ in order to reduce the effect of the container walls to less than 1%.

Case B-2. Almost steady rotation.—When the penetration depth becomes comparable to or larger than the distance between the disk and the stationary container, the velocity distribution in the liquid approaches that of a steady state condition; the inertial terms due to acceleration of the liquid become much smaller than those due to viscosity. The damping tends to become almost solely dependent on the viscosity, rather than on the product of viscosity and density. Evaluating the torques on the faces and the edge from Eq. (18), we obtain

$$\eta = \left(\frac{2I\delta}{a^2\tau\lambda}\right)\left(\coth\epsilon + \frac{d}{a}\coth\sigma\right)^{-1},$$

where

$$\epsilon = (h-d)/\lambda, \quad \sigma = (b-a)/\lambda, \tag{20}$$

where $(b-a) \ll a$. For small ϵ, σ, Eq. (20) approaches the case of steady rotation, as demonstrated by expanding $\coth\epsilon$ and $\coth\sigma$;

$$\eta = \frac{2I}{a^3\tau}\left[\left(\frac{a}{h-d}\right)\left(1 + \frac{\epsilon^2}{3} - \frac{\epsilon^4}{45} + \cdots\right) + \left(\frac{d}{b-a}\right)\left(1 + \frac{\sigma^2}{3} - \frac{\sigma^4}{45} + \cdots\right)\right]^{-1}. \tag{21}$$

Corner Correction

We have been treating the motion of the fluid as if it were stirred by the independent action of two faces and the edge of the disk. This simplification permitted a reduction of the two-dimensional Navier-Stokes equation which has a singularity at the intersection of the face and edge surfaces, to two one-dimensional equations, which are regular everywhere. This method of approximation is equivalent to determining the liquid velocity distribution in the z direction produced by the torsional oscillations of a disk of infinite radius and then the drag of the liquid upon a central circular (radius a) section of the infinite disk. The radial solution was correspondingly equivalent to taking a short length d of an infinitely long cylinder of radius a. The pieces of the infinite surfaces were then added together to

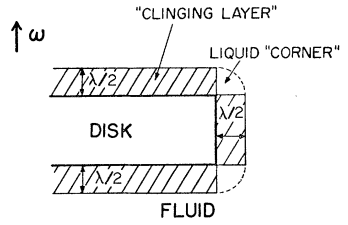

FIG. 1. Schematic representation of boundary layer in the neighborhood of the disk corner.

represent a finite disk. We shall presently show that this approximation suffers from at least one important defect and then describe a semiempirical method for removing it.

By approximating $(1+\delta)^{\frac{1}{2}}=1$, Eq. (17b) can be interpreted as stating that the moment of inertia of the disk is increased by an amount equivalent to a fluid layer $\lambda/2$ thick that clings to the disk surface;

$$I(\tau^2/\tau_0^2-1)=\rho(\lambda/2)\pi a^4(1+2d/a^4)\equiv I_\lambda. \quad (22)$$

Rearranging terms in Eq. (17a) and approximating $(1-\delta)^{\frac{1}{2}}=1$, $3\lambda d/a^2=0$, $\tau^2/\tau_0^2+1=2$, we obtain

$$\delta=\frac{\rho\lambda\pi a^4(1+2d/a)}{4I}=\frac{I_\lambda}{2}, \quad (23)$$

where I_λ is the moment of inertia of the "clinging layer" determined above. Referring now to Fig. 1, we have attempted to pictorialize the "clinging layer" in the neighborhood of the disk corner. The diagram shows a fluid region that was completely neglected in the infinite surface section approximation. According to this simple picture, the "neglected corner" extends radially $\sim\lambda/2$ beyond the disk radius and also axially $\sim\lambda/2$ above the plane surface of the disk. The corner then has a cross-sectional area proportional to λ^2; we let its cross section be equal to $\nu\lambda^2$, where ν is the "corner parameter." The upper and lower liquid corners therefore have a moment of inertia $I_c=4\pi a^3\rho\nu\lambda^2$. Assuming that the corners exert an influence upon the disk in a manner similar to that of the fluid adjacent to the plane and circular surfaces, the total moment of inertia added by the fluid becomes

$$I(\tau^2/\tau_0^2-1)=I_\lambda+I_c, \quad (24)$$

and the total decrement

$$\delta=(I_\lambda+I_c)/2I. \quad (25)$$

Finally, retracing the steps by which we arrived at these simple representations and restoring the correction terms, we obtain the "corrected" equations corresponding to Eqs. (17a, b);

$$\mathrm{Re}\,[(\eta\rho)^{\frac{1}{2}}]=\frac{2I\delta(\tau^2/\tau_0^2+1)}{a^4[\pi\tau(1-\delta)]^{\frac{1}{2}}(1+2d/a+3\lambda d/a^2+8\nu\lambda/a)}, \quad (26a)$$

$$\mathrm{Im}\,[(\eta\rho)^{\frac{1}{2}}]=\frac{2I(\tau^2/\tau_0^2-1)}{a^4[\pi\tau(1+\delta)]^{\frac{1}{2}}(1+2d/a+8\nu\lambda/a)}. \quad (26b)$$

The calculation just carried out is not rigorous, for the effect of the corner must perturb the velocity profile some finite distance into the previously calculated plane and cylindrical surface regions. The calculation does, however, offer a tractable functional dependence for the effect of the corner, which is expressed in terms of the parameter ν. Furthermore, it is possible to obtain an experimental determination of the effect. Oscillating-disk studies in a medium whose viscosity and density are known (the viscosity having been measured by different, and presumably less theoretically difficult methods) will yield data that may be solved for ν directly. Dilute gases are well suited for such a calibration, for their viscosities are quite independent of density over a wide range, and the penetration depth can be varied by changing the pressure. The parameter may also be determined by comparing the results obtained from two different torsion pendulum studies of the same fluid. Either the disk radii or the oscillation periods should be significantly different in order to compare the fluid viscosities derived from systems having different ratios λ/a.

Constancy of the parameter ν over a wide range of λ should indicate that one has a satisfactory functional dependence for the effect of the neglected corner.

Influence of the Suspension

We now extend the problem of an idealized pendulum to take account of the dissipative terms beyond those due to the disk alone.

In common practice the disk is attached to a stiff rod which hangs from a torsion fiber; the disk and the lower portion of the rod are immersed in the liquid, while the upper portion of the rod is surrounded by vapor at the equilibrium vapor pressure of the liquid. The upper portion of the rod carries a plane mirror for the purpose of determining the periods and deflection angles. The torsion fiber has some measurable internal friction. The total "nuisance damping" decrement δ_0 results from all these dissipative terms, but experimental determinations of δ_0 are usually carried out with the pendulum in high vacuum, a procedure which can only measure the effect of the fiber friction. Unless it is possible to establish that the rod and mirror terms are negligible, this practice may cause appreciable errors in the liquid helium data at low temperatures, where the δ due to the liquid around the disk is small.

The torque due to the liquid around the lower portion of the rod is given by the previously calculated drag on the cylindrical edge of the disk, if the rod radius a' and immersion depth d' are substituted for a and d. Defining δ_0' as the nuisance decrement due to all torques other than those of the liquid, we obtain, after Eq. (26a),

$$\mathrm{Re}\,[(\rho\eta)^{\frac{1}{2}}]=\frac{2I[\delta(\tau^2/\tau_0^2+1)-2\delta_0'\tau/\tau_0]}{a^4[\pi\tau(1-\delta)]^{\frac{1}{2}}(1+2d/a+2d'a'^3/a^4\times(3\lambda d/a^2)+3\lambda d'a'^2/a^4+8\nu\lambda/a)}. \quad (27)$$

Comparison between the results of two different disks attached alternately to the same suspension and oscillating in the same fluid can yield an experimental measurement of δ_0'. The disks should be designed to have significantly different decrements in the fluid; if the viscosity and density of the liquid are known, the right-hand sides of Eq. (27) (with the appropriate values pertinent to the two disks and the suspension) can be equated, and δ_0' solved directly.

Finned Rotor

Although a single disk experiment will not in itself yield the values of ρ and η individually, the single disk may be replaced by a rotor whose interaction with the liquid has a markedly different dependence on the penetration depth. Simultaneous solutions of the equations proper to the two oscillating systems may then yield ρ and η separately. An analytically simple secondary rotor satisfying the requirements is a coaxial array of closely-spaced plane disks which are made to oscillate as a unit.

We consider $N+1$ plane circular disks, each of radius a_1 and thickness d, separated normal to their planes by washers of radius a_2 and thickness $2s$. The total moment of the assembly is I. The solution of the hydrodynamic equation for the exposed top and bottom faces and the $N+1$ edges is given by the single disk formulas. The motion of the liquid laminae between the plates is obtained by applying the new boundary conditions to the general axial solution, Eq. (12). For an origin midway between two plates, we have

$$Z=\cosh pz/\cosh ps.$$

Calculating the corresponding torque in the conventional way, the N liquid laminae contribute a torque,

$$(K\dot{\theta})_{\text{laminae}}=\frac{N\pi\eta\dot{\theta}}{\lambda}(a_1^4-a_2^4)[(1-\delta)^{\frac{1}{2}}+i(1+\delta)^{\frac{1}{2}}]\times\frac{\sinh[2s(1-\delta)^{\frac{1}{2}}/\lambda]+i\sin[2s(1+\delta)^{\frac{1}{2}}/\lambda]}{\cosh[2s(1-\delta)^{\frac{1}{2}}/\lambda]+\cos[2s(1+\delta)^{\frac{1}{2}}/\lambda]}. \quad (28)$$

Adding the torque due to the laminae to that due to the exposed surfaces, and approximating $(1+\delta)^{\frac{1}{2}}=1$, we obtain the real and imaginary equations

$$\text{Re}\,[(\rho\eta)^{\frac{1}{2}}]=\frac{2I}{(\pi\tau)^{\frac{1}{2}}}\left[\frac{\delta(\tau^2/\tau_0^2+1)-2\delta_0\tau/\tau_0}{N(a_1^4-a_2^4)F_1+a_1^4+2(N+1)da_1^3+8\nu(N+1)\lambda a_1^3+3(N+1)\lambda da_1^2}\right], \quad (29a)$$

$$\text{Im}\,[(\rho\eta)^{\frac{1}{2}}]=\frac{2I}{(\pi\tau)^{\frac{1}{2}}}\left[\frac{\tau^2/\tau_0^2-1}{N(a_1^4-a_2^4)F_2+2(N+1)da_1^3+8\nu(N+1)\lambda a_1^3+a_1^4}\right], \quad (29b)$$

where

$$F_1=\frac{\sinh(2s/\lambda)-\sin(2s/\lambda)}{\cosh(2s/\lambda)-\cos(2s/\lambda)},\qquad F_2=\frac{\sinh(2s/\lambda)+\sin(2s/\lambda)}{\cosh(2s/\lambda)+\cos(2s/\lambda)}.$$

Equations (29) become incorrect when $\lambda\leq\sim s$, due to an overestimate of the corner correction, since the calculated liquid corners of adjacent plates begin to overlap. It is apparent that the real rotor cannot drag more liquid than if the entire assembly of plates were enclosed in a thin smooth sheath. We then impose such a condition as an upper limit on the radial boundary layer effect, obtaining for the case of $\lambda\geq\sim s$,

$$\text{Re}\,[(\rho\eta)^{\frac{1}{2}}]=\frac{2I}{(\pi\tau)^{\frac{1}{2}}}\left[\frac{\delta(\tau^2/\tau_0^2+1)-2\delta_0\tau/\tau_0}{N(a_1^4-a_2^4)F_1+a_1^4+2Ha_1^3+8\nu\lambda a_1^3+3H\lambda a_1^2}\right], \quad (30a)$$

$$\text{Im}\,[(\rho\eta)^{\frac{1}{2}}]=\frac{2I}{(\pi\tau)^{\frac{1}{2}}}\left[\frac{\tau^2/\tau_0^2-1}{N(a_1^4-a_2^4)F_2+a_1^4+2Ha_1^3+8\nu\lambda a_1^3}\right], \quad (30b)$$

where $H=2Ns+(N+1)d$ is the total height of the assembly. As the penetration depth increases further, $F_1\to 0$ and $F_2\to 2s/\lambda$. In this limit, the damping Eq. (30a) is equivalent to that of a single disk of thickness H, while the imaginary Eq. (30b) states that the moment of the rotor is increased by the total moment of the liquid contained between the plates plus the layer clinging to the outside surface, for Eq. (30b) can be rewritten in the form,

$$I(\tau^2/\tau_0^2-1)=\tfrac{1}{2}\pi\rho[2sN(a_1^4-a_2^4)+\lambda(a_1^4+2Ha_1^3+8\nu\lambda a_1^3)]. \quad (31)$$

Experimental Determination of Corner Correction

We have measured the corner parameter ν over a wide range of experimental conditions, according to a procedure outlined in a preceding section. Solving the single disk Eq. (27) for ν, we obtain

$$\nu=\frac{a}{8\lambda}\left\{\frac{a^4[\eta\rho\tau(1-\delta)]^{\frac{1}{2}}}{2I[\delta(\tau^2/\tau_0^2+1)-2\delta_0\tau/\tau_0]}-\left(1+\frac{2d}{a}+\frac{3\lambda d}{a^2}\right)\right\}.$$

Observations of the period and decrement of oscillations

TABLE I. Experimental corner parameters.

Fluid	τ_0 sec	η micropoise	ρ g/cm³	λ/a	ν
He gas, 75°K	6.775	79	0.605×10^{-4}	0.674	0.33
			1.31	0.458	0.33
			2.41	0.337	0.30
			4.96	0.234	0.32
Air, 22°C	42.07	182.4	9.21×10^{-4}	0.652	0.31
	6.775		9.28	0.255	0.29
N_2 vapor, 75° K	6.775	52.4	5.51×10^{-4}	0.202	0.28
			11.78	0.124	0.43
			22.4	0.0896	0.34
			35.3	0.0716	0.37
Water, room temp.	14.669	9185	0.9973	0.0394	0.31
	9.900	9081	0.9972	0.0320	0.37
	5.095	9336	0.9975	0.0234	0.46
			Average, $\bar{\nu}=0.34$		±0.04

of a disk in a medium of known viscosity and density directly yield the value of the parameter.

The first series of measurements were carried out with the thin Dural disk described in Sec. III of this paper. The first medium studied was dry air, whose viscosity has been determined by Bearden[10] by means of a rotating cylinder viscometer. Our studies in air were carried out at two oscillation periods, obtained by suspending the pendulum alternately from 25-cm lengths of 0.0076-cm diameter platinum wire, and 0.0025-cm diameter tantalum wire. These fibers gave vacuum periods of 6.775 and 42.07 seconds, respectively, and in air yielded penetration depths of one-quarter to more than one-half of the disk radius. Although the values $\nu=0.29$, 0.31 for the two periods agree closely, these λ/a ratios were too large to form the basis for a conclusion about the value of ν for much smaller λ/a. Furthermore, it was desirable to measure ν in media having different viscosities and densities. Accordingly, we determined the corner effect with the Dural disk in N_2 and He vapors at 75°K. The viscosity of He gas was obtained by extrapolating the measurements of Johnston and Grilly,[11] whose studies of a thin disk oscillating between closely-spaced stators extended down to 80°K. The density was calculated as that of an ideal gas and was varied by changing the pressure. The value of the corner parameter given by the He at four pressures was $\nu=0.32\pm0.01$, for a λ/a range of 0.23–0.67. Measurements in N_2 vapor were based upon the viscosity extrapolated from the data of Johnston and McCloskey,[12] whose studies ranged from 90–300°K. The density was calculated using the second virial coefficient.[13] Measurements at four pressures yielded $\nu=0.35\pm0.05$, for a λ/a range of 0.07–0.20.

The second series of measurements were made with a large disk in water. The disk was turned from a single block of stainless steel ($\rho=7.8948$ g/cm³) to a radius of 5.2984 cm and a thickness of 1.2085 cm. It was soldered to a 30-cm length of 0.238-cm diameter steel rod and suspended by various lengths of 0.041-cm diameter steel music wire. The moment of inertia of the pendulum was computed to be 1.1812×10^4 g cm². Although it was not possible to measure the nuisance decrement, the observations in air gave a decrement of 2.4×10^{-4}, approximately 2% of the decrement in water. The nuisance decrement could therefore be ignored. Similarly, the vacuum period was taken as the period of the disk in air. The disk was immersed in degassed distilled water contained in a cylindrical glass reservoir of 29-cm internal diameter. The temperature of the water was measured to 0.1°C with a mercury thermometer. Viscosity values of the water were taken from a study of Poiseuille flow by Bingham and Jackson.[14] Measurements at three oscillation periods yielded an average $\nu=0.38\pm0.06$ over a λ/a range of 0.023–0.032.

There is no significant trend of ν with any of the parameters λ/a, ρ, or η. Although the viscosity of water is probably known to the highest accuracy of the four fluids studied, the water measurements show the greatest mean deviation, demonstrating the loss in experimental sensitivity when the correction term $8\nu\lambda/a$ is small. The determination in air, on the other hand, suffers to some extent due to the large magnitude of the correction, since the moment of inertia of the "neglected corner" was originally assumed to be that of a thin ring. Finally, the viscosities of the He and N_2 are extrapolations of measured values. We have taken the arithmetical average of the set as the best value of ν. The same average $\nu=0.34\pm0.04$ is obtained with equal weight on each of the 13 separate determinations or with equal weight to the average of each of the 4 fluids. Data for the individual determinations are given in Table I.

Review of Theory

Modern studies of "nearly infinite" viscous media by means of the torsion pendulum have been based upon Meyer's[15] analytic solutions of the right circular cylinder. Since these solutions lead to a correction term that is different from the "corner effect," we shall discuss Meyer's theory. Starting with the Navier-Stokes equation and the same assumptions of the liquid flow pattern as adopted here, Meyer obtained a radial distribution equation in agreement with Eq. (9a). His

[10] J. A. Bearden, Phys. Rev. **56**, 1023 (1939).
[11] H. L. Johnston and E. R. Grilly, J. Phys. Chem. **46**, 948 (1942).
[12] H. L. Johnston and K. E. McCloskey, J. Phys. Chem. **44**, 1038 (1940).
[13] A. S. Friedman, dissertation, Ohio State University, 1950 (unpublished).
[14] E. C. Bingham and R. F. Jackson, J. Research Natl. Bur. Standards **14**, 59 (1918).
[15] O. E. Meyer, Ann. Physik **32**, 642 (1887).

equation for the axial distribution, however, is given as

$$\frac{d^2Z}{dz^2}+\frac{4}{a}\left(\frac{dR}{dr}\right)_{r=a}-p^2Z=0,$$

which differs from Eq. (9b) by the inclusion of the second term. It originates from Meyer's consideration of the motion of the fluid within the region $r\leq a$ as if composed of disk-like laminae of infinitesimal thickness, and the evaluation of torques on the laminae.[16] The drag on each fluid plate was given as the sum of torques on the upper and bottom faces, and on the cylindrical edges, as if the fluid disk were solid. The contribution due to the faces appears to be valid for the case of infinitesimal thickness, but the assumption of a torque due to the disk edge does not appear to be justified. The lamina cannot support a shearing stress without rapid attenuation in a distance of the order of the penetration depth, which is presumed to be smaller than the disk radius. (Although it is obvious that the fluid laminae must suffer angular shearing distortion in the region $r<a$, this has been neglected in the present approximation. The apparent constancy of the empirical corner parameter seems to justify the present approach.) The addition of the hypothetical "edge torque" of Meyer results in the second term of the above differential equation. Calculation of the resulting equations of motion of a single oscillating disk leads to formulas similar to those given in this paper, such as Eq. (27), with the exception of the term $2\lambda/a$, which replaces the corner correction $8\nu\lambda/a$. Although the functional dependence is the same for both, our experimental value of the parameter yields a coefficient $8\nu\simeq 2.7$, about 35% higher than that given by Meyer.

Meyer's differential equations have apparently formed the basis of analysis of the oscillating disk investigations of liquid helium that were performed by Keesom and MacWood,[2] Andronikashvili,[3–5] de Troyer, van Itterbeek and van den Berg,[6] and Hallett.[7] The first authors used equations derived by MacWood; mistakes in intermediate steps resulted in formulas quite different from those derived in the present paper. Hallett has presented a brief discussion of these errors. The latter three groups of investigators have used essentially the same disk formulas, derived independently. Of these papers, only Hallett has published a derivation. The final equations contain the "Meyer term" $2\lambda/a$, and do not include the term $3\lambda d/a^2$, which arises from the derivative of the radial velocity distribution. It is apparent that both terms tend to become unimportant when λ/a is sufficiently small. They are not insignificant in the liquid helium work; furthermore, there is a measurable effect caused by replacing Meyer's coefficient with our empirical correction. For example, typical values encountered in the single disk studies are ratios $\lambda/a\simeq 0.015$ at the lambda point ($\tau=10$ sec, $\rho=0.145$ g/cm^3, $\eta=28$ micropoise, $a=2$); at lower temperatures the decreased normal fluid density causes λ/a to increase by a factor of about three at 1.2°K. At the lambda point, the product $\rho\eta$ calculated on the basis of the Meyer correction is approximately 2% higher than if one uses the empirical coefficient. The discrepancy rises to 6% at the lower temperature. Under certain circumstances, the error can be considerably larger. Hallett obtained his "disk constant" $4I^2/\pi a^8$ by a calibration procedure in air at room temperature. He used the Meyer correction and neglected the radial term $3\lambda d/a^2$. The calibration value of the disk constant thus obtained is 28% lower than that calculated directly from the density, thickness, and radius of the disk. A recalculation of the air calibration, using Eq. (27) and the empirical corner parameter, reduces the disagreement to about 6%.

Certain motions that deviate from the idealized flow pattern have not been considered. In addition to the already mentioned angular shear in the region $r<a$, we have neglected velocity terms of higher order than the first, of which centrifugal flow is a result, and effects due to the failure of the disk to execute purely torsional oscillations in its own plane. Higher order velocity terms become more important as the velocity of the disk is increased, and cause the oscillations to decay with an exponent that is a function of the amplitude. Hence, the applicability of the equations may be tested by observing the oscillations over an amplitude range sufficiently large to detect a significant variation in the decrement. Nonideal motion of the disk system, caused by an angular or translational displacement of the rotation axis, dissipates energy by compression waves transmitted to the liquid. These unwanted motions may be detected by visual observation.

III. EXPERIMENTAL DETAILS

Cryostat and Thermometry

The experiments on pure He^4 were carried out in a large cryostat which is shown schematically in Fig. 2. The He Dewar B has an internal diameter of 93 mm and a vacuum-jacketed internal length of 800 mm. During the greater part of this investigation, the liquid nitrogen Dewar was supported on a thrust bearing, so that it could be rotated until the unsilvered vertical stripe of the inner Dewar was well shielded from room temperature radiation. The torsion head assembly consists of a $4\frac{1}{2}$-in. long section of 3-in o.d.$\times\frac{1}{8}$-in. wall cylindrical Lucite tubing W, a section of brass tubing of the same diameter, and a vacuum-tight $\frac{1}{4}$-in. diameter shaft "O-ring" seal S. The He Dewar and the torsion head are assembled at the joints J with bolted "O-ring" seals, which permit rapid removal and installation of different oscillating systems. The pendulum

[16] R. D. Glauz (private communication). The authors are indebted to Dr. Glauz for drawing our attention to the source of Meyer's error.

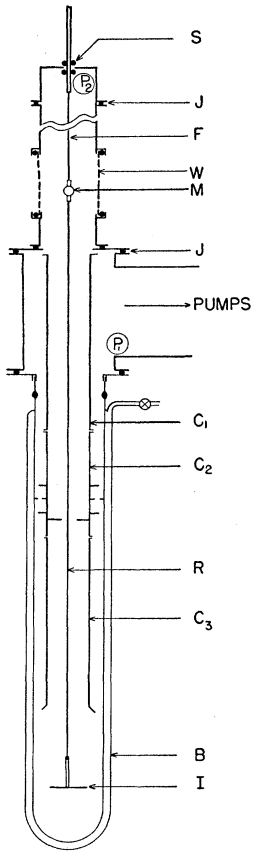

FIG. 2. Schematic of the experimental apparatus.

consists of an inertial body I, which is suspended from a stiff rod R and a torsion fiber F. The radiation shield consists of three sections C_1, C_2, C_3 of thin-walled stainless steel tubing of 62-mm diameter. It is provided with radiation baffles in the annular space adjacent to the Dewar wall and an internal removable shield which has a central 16-mm hole to permit passage of R. The apparatus was carefully shielded from mechanical vibrations.

Vapor pressure of the liquid helium is measured by mercury and butyl sebacate manometers connected to the cryostat at P_1 and P_2. In order to obtain high sensitivity and accuracy in the pressure measurements, we conducted a density determination of degassed butyl sebacate at several temperatures between 22°C and 26°C; the sample used in the manometers has a density of $0.93190[1+0.000835(25-t)]$ g/cm^3, where t is the centigrade temperature. Oil manometer measurements are converted to mercury level differences, using a factor composed of the density of mercury at 20°C, the density of the butyl sebacate, and the gravitational accelerations at Los Alamos and at sea level. Temperatures of the liquid helium are given according to the "1955 E" vapor pressure scale.[17] In later sections of this paper we discuss some helium measurements carried out by other investigators; their published temperatures have been converted to the "1955 E" scale. Temperatures of the liquid helium are stabilized by an electronic regulator[18] to within 0.2-mm oil, the accuracy to which the manometers are read. This corresponds to temperature uncertainties of about 2×10^{-4} °K near the lambda point, and 2×10^{-3} °K at 1.2°K.

Measurement of Period and Amplitude

Optical Lever

Angular position of the pendulum is determined by a light beam reflected from the mirror M on to an engraved cellulose acetate scale held in a circular arc of approximately 26-cm radius with its center at M. The light source is a battery powered General Electric Company 835 lamp, which has a straight single filament of approximately 0.05-mm diameter wire. The reflected image of the filament is focused through a small aperture lens upon the curved scale. Magnification of the lamp system is approximately 7; the width of the projected filament image is about 0.5 mm.

The system is set into torsional oscillations by imparting a temporary angular deflection to the shaft. The pendulum's angular position at rest is maintained by a lever clamped to the upper part of the torsion head shaft, and a mechanical stop. The rest position of the pendulum reproducibly coincides with the zero mark on the scale to within the angular width of the filament image. Alignment of the pendulum components is in all cases adequate to preclude any evidence of eccentric oscillations or of a gravitational pendulum. Since the mirror was concentric with the window, there were no corrections for refraction of the light beam.

Chronometry

Determination of the oscillation periods is performed with the aid of a photosensitive detector placed at the rest position of the light beam on the scale, and an electronic chronograph. The photosensitive detector is a Western Electric Company Model 1740 *p-n* junction germanium photodiode having a sensitive aperture measuring 0.5 mm wide by 1.0 mm high and a sensitivity of 10 microamperes/millilumen. The narrow light beam sweeping across the face of the diode produces a transient increase in conductivity. This conduction pulse is converted by a stable dc bridge and amplifier into a strong voltage pulse which is fed to a chronograph. The timing circuit of the chronograph is controlled by a 100-kc crystal oscillator. Four scaler strips and a digital register display elapsed time with a precision of 0.1 millisecond. The scaler strips are started by a bi-stable multivibrator, or flip-flop circuit, actuated by a 7-volt pulse from the detector amplifier, and are stopped by a pulse supplied to the other side of the

[17] Clement, Logan, and Gaffney, Phys. Rev. **100**, 743 (1955); see their "Note added in proof."

[18] H. S. Sommers, Jr., Rev. Sci. Instr. **25**, 793 (1954).

flip-flop circuit. In typical operation, periods are timed by closing the switch leading to the "start" side of the flip-flop circuit shortly before a transit of the light beam across the detector. When the beam crosses the detector, the resulting pulse starts the chronograph; as long as the switch is in the "start" position, the timing circuits continue to run. The number of transits of the beam across the photodiode is indicated by a separate digital register. After the pendulum has performed a suitable number of cycles, the switch is thrown to the "stop" position and the next transit of the beam provides a pulse to the side of the flip-flop circuit that halts the choronograph. Final display of the timing measurement therefore includes the total elapsed time, to 0.1 millisecond, for the recorded number of half-cycles. Measurements are made only for an even number of half-cycles.

Frequency of the crystal controlling the chronograph and its drift during warmup are determined by comparison with a standard crystal oscillator which has been calibrated to within 3 parts in 10^6 with signals from the National Bureau of Standards broadcasting station *WWV*. The warmup drift is approximately 10 cps during the first three hours after which the frequency does not vary by more than 0.5 cps. During density measurements, the chronograph is continuously compared with the standard oscillator by means of a Hewlett-Packard Frequency Counter, and periods of the pendulum are corrected for deviations of the chronograph from a reference frequency of 100 035 cps.

Timing Corrections and Fiber Characteristics

The finite width of the light beam causes a systematic error in the triggering of the chronograph. Taking the peak of the voltage pulse as the true zero of the pendulum, the chronograph is turned on and off too early, by an interval corresponding to the transit time of the half width of the electrical pulse. Although the "pretriggering" error at the start of a timing run tends to cancel the error at the end, the lower amplitude of oscillation, and hence, beam transit velocity, at the end of the run causes the "stop" pulse error to be larger. The error is reduced considerably by a dc bias applied to the output of the amplifier, so that the chronograph is turned on and off only near the peak of the pulse. A fast oscillograph inspection of the amplifier output showed that biasing reduces the effective electrical pulse width to about 0.1 mm. The pretriggering effect causes errors in the same direction as those due to the failure of the fiber to obey Hooke's law. In order to determine the combined effects of pretriggering and deviations from Hooke's law, we studied the variation of period with amplitude for tantalum fibers. The coefficient of amplitude dependence was found to be $(1/\tau)(d\tau/d\theta)=1.85\times10^{-4}$ rad^{-1} up to an amplitude of 0.3 radian, which was the upper limit of amplitudes employed in the He II studies. The finite damping of oscillations causes an increase in period over the undamped value by an amount $\Delta\tau/\tau\simeq\delta^2/2$. Maximum damping of the pendulum occurs in the neighborhood of the lambda point, where $\delta\simeq10^{-2}$. The combined effects of finite pulse width, anharmonicity of the fiber, and damping of oscillations upon the period cause errors which do not exceed 3 milliseconds in the present studies. The data are not corrected for these effects.

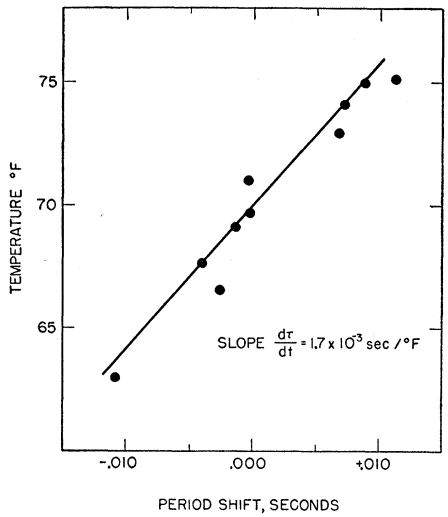

FIG. 3. Variation of rotor period due to temperature dependence of the torsion constant of the tantalum suspension fiber.

In the case of the finned rotors suspended from tantalum fibers, variations in room temperature caused noticeable changes in the measured periods. An investigation of this dependence yielded a linear coefficient $(1/\tau)(d\tau/dt)=4.6\times10^{-5}$ (°F)$^{-1}$ between 65 and 75°F, as shown in Fig. 3. Since the rotor was shielded from temperature fluctuations by a good vacuum in the inner Dewar during this investigation, the coefficient was ascribed to the temperature dependence of the torsion constant of the tantalum fiber. Published measurements of the temperature coefficient of the elastic modulus of tantalum[19] quote a value within 20% of that derived from our study. All rotor periods were therefore corrected, by means of the above coefficient and a thermometer in contact with the torsion head, to a constant fiber temperature.

Oscillating Disk Systems

A. Thin Single Disk

A thin circular disk (L) of Duralumin, shown schematically in Fig. 4A, was studied in order to obtain the principal data for a calculation of the product $\rho\eta$ in pure He^4, according to Eq. (27). The disk was turned from a rod of Duralumin, whose density was determined by measurements of the dimensions and mass of a large sample length cut from the same rod. The measured

[19] V. W. Köster, Z. Metallkunde **39**, 1 (1948).

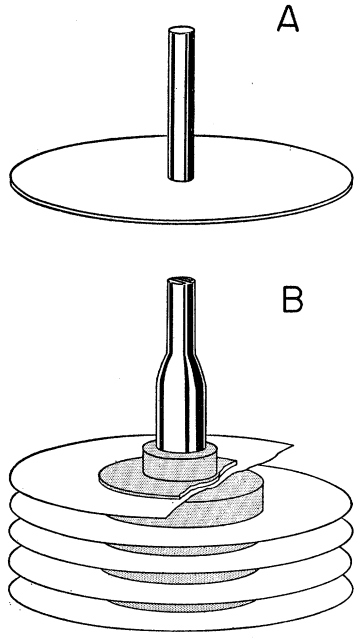

FIG. 4. Design of the oscillating disk systems.

characteristics of the disk are: density, 2.796 g/cm^3; disk radius a, 2.500$_6$ cm; disk thickness d, 0.0500$_4$ cm; stem radius a', 0.0824 cm; and stem length d', 2.54 cm. The computed moment of inertia of Disk (L) is 8.821 g cm^2 at room temperature.

The disk was cemented to the lower end of a solid fused quartz rod of 0.9-mm diameter and 108-cm length. The torsion fiber was a 25-cm length of 0.0076-cm diameter hard-drawn platinum wire, clamped at its upper end to the shaft S, and cemented at its lower end to the quartz rod. The mirror was a front-surface-aluminized piece of 0.03-mm thick microscope cover glass, measuring 12 mm high and 4 mm wide. Rod and mirror had a computed moment of inertia of 0.0302 g cm^2. The disk was suspended on the axis of the Dewar and approximately 10 cm above the bottom of the Dewar. The liquid region extended away from the disk at least 2 cm in each direction.

During experiments with Disk (L), the tubing shield consisted of Sec. C_2 only.

B. Finned Rotors

In order to obtain the principal data for calculation of density according to Eq. (30b), a finned rotor ($L1$), shown schematically in Fig. 4B was constructed in a design similar to that used previously.[3,4,7] One hundred circular disks of Dural of nominally 0.001-in. thickness and 2-in. diameter were interleaved with 99 aluminum washers 0.008-in. thick and 1-in. in diameter on a Dural mandrel passing through a center hole in each disk, and clamped in a rigid stack by a sliding collar and Dural pin through the collar and mandrel. The Dural disks and the aluminum washers were turned, drilled, and bored while compressed in stacks of 50–150 sheets. Average densities and thicknesses were determined by weighing and measuring the completed stacks. This procedure insured the cancellation of errors due to fluctuations of density and thickness for a calculation of moments of inertia. Dimensions of the Dural disks are outer radius, 2.5381 cm; inner radius, 0.3175 cm; thickness, 0.002777 cm; and moment (100 disks), 49.480 g cm^2. Dimensions of the aluminum washers are outer radius, 1.271 cm; inner radius, 0.3188 cm; thickness, 0.1971 cm; and moment (99 washers), 21.519 g cm^2. Measured mass of the assembled rotor is 46.752 g. Average separation between disks was determined by measuring the total height of the disks and washers after final assembly, to be 0.02001 cm. The moments of the collar and mandrel are 0.7150 g cm^2 and 0.8895 g cm^2, respectively.

The suspension rod was a 108-cm length of Monel tube of 0.16 cm o.d. and 0.0076-cm wall thickness, at the lower end of which was soldered a 0–80 screw which fitted a tapped hole in the mandrel. The calculated moment of the rod, fiber clamp, and mirror was 0.2251 g cm^2. The suspension fiber was 0.005-cm tantalum, 26 cm long.

Since the accumulation of small errors in measurement of the dimensions of the components could lead to an appreciable error in the calculated moment of the rotor, we determined the moment by a comparison method. A thick single disk of very nearly the same moment and mass of Rotor ($L1$) was turned from a single block of Dural of measured density. Its period of oscillation in vacuum at room temperature when attached to the same rod and fiber was compared with the period of the rotor. The moment of Rotor ($L1$) was thus determined to be 72.336 g cm^2, which disagrees by 0.37% with the value obtained by summing the contributions of the rotor components. Since the moment of the "standard" thick disk was calculated from only four dimensions and one mass and since the measured periods of the standard disk and of the rotor had mean deviations of less than 2 parts in 10^4, the comparison value of the rotor moment is more reliable. We therefore take as the moment of Rotor ($L1$) and suspension at room temperature, the value 72.561 g cm^2.

Initial studies with Rotor ($L1$) were carried out with radiation shield C_2, as used in the Disk (L) work. This particular assembly of Rotor ($L1$), suspension fiber, and radiation shield is designated as Rotor ($L1$A), and experimental results obtained with Rotor ($L1$A) are labeled accordingly.

Experiments carried out with Rotor ($L1A$) in the low vapor pressure range of liquid helium indicated that motion of vapor toward the pumping line exerted a significant effect on the pendulum periods and the rest position. This effect was verified by introducing a source of gas into the cryostat at room temperature in order to simulate the efflux of vapor to the pump. A

simple analysis and the simulated effect showed that the interaction between the moving vapor and the suspension is greatest at low pressure, for constant mass flow rate of gas. At pressures above that corresponding to 1.5°K, the effect was too small to be significant. Accordingly, the experiments with Rotor ($L1A$) were repeated with the Rotor ($L1$) and the shield C_1, C_2, C_3, which insured that the suspension was surrounded with a static gas column. In addition, modifications in the suspension clamp and mirror, and use of a new tantalum fiber require us to designate this second pendulum assembly as Rotor ($L1B$). The total moment of inertia in this case was 72.353 g cm².

The design of Rotor ($L1$), involving thin disks and narrow gaps between the disks, was necessitated by the requirements of negligible slippage of viscous fluid and relatively low moment of inertia. The separation between plates was sufficient to cause 99.9% of the fluid to be dragged at the lambda point, as discussed later. The thin vanes of the rotor were, however, slightly warped; when viewed on edge, some of the disks touched adjacent ones at the periphery. The oscillations of Rotor ($L1$) were therefore not purely shear vibrations, and could set a small portion of superfluid into motion. The effect of the imperfect motion was to cause a fictitious increase in deduced values of viscous fluid density, the increase being proportional to the density of superfluid. A Rotor ($L2$) was constructed specifically for studies in the region of low normal fluid density. Its design was based upon the known increase of kinematic viscosity of He II at low temperatures, permitting the use of larger plate separations. Thickness and separation between disks were roughly five times those of Rotor ($L1$); the number of plates was reduced to 21. In order to minimize warpage, the disks were turned from flat, stress-relieved Dural. The assembled stack was installed in a closely fitted thin-walled cylindrical sheath, which eliminated the necessity for estimating the smoothness of the cylindrical boundary layer. Other construction details were similar to the original rotor. Specifications of the major components are: disks of 2.5400-cm radius, 0.0135 cm thick; washers of 1.270-cm radius 0.08009 cm thick; cylindrical sleeve of 1.915-cm height, 2.540-cm internal radius, 0.00553-cm wall thickness. The regularity of the assembled rotor was examined by rotating it in a lathe before adding the sheath; the disks appeared to be plane to within 0.003 cm. Total moment of inertia of the Rotor ($L2$), sheath and suspension was computed to be 79.322 g cm². It was installed in the cryostat in conjunction with radiation shield and baffle C_1 and C_2.

Measurement of Vacuum Periods and Decrements

The vacuum periods τ_0 of Rotors ($L1A$) and ($L1B$) at liquid He temperatures were not measured directly. They were obtained by measurements of the vacuum periods at room temperature and at 75°K, and an extrapolation to liquid He temperature using the following procedure. In order to insure that the rotor reached liquid nitrogen temperature, He gas was admitted to the inner Dewar space and to its annular jacket, and the outer Dewar was filled with liquid nitrogen. Since the He gas in the inner Dewar was required for thermal equilibrium but made an unwanted contribution to the period of the rotor, we measured periods as a function of gas pressure over the range 55—2 mm Hg. These periods, plotted *versus* pressure, fell on a smooth curve and were extrapolated to the value at zero pressure, as shown in Fig. 5. The change from the value in high vacuum at room temperature yielded a fractional effect $\Delta\tau/\tau(294-75°\text{K})=3.78\times10^{-3}$. This ratio is equal to the total contraction coefficient of the rotor material: $\Delta\tau/\tau=\Delta r/r=\int_{75}^{294}\alpha dT$, where α is the differential thermal coefficient of expansion. Independent measurements[20] of the α of pure aluminum yield the integrated coefficient $\Delta r/r=3.81\times10^{-3}$ for the same temperature change, and 0.2×10^{-3} for the residual coefficient from 75°K to 4°K. In view of the excellent agreement between these data for the range 294–75°K, we accepted the value for the residual change as representative of the contraction of the Dural rotor and disk from liquid nitrogen to liquid helium temperature. The corresponding reduction in the period of the rotor was about 7 milliseconds below that at 75°K. We thus obtained for the vacuum periods at 4°K: Rotor ($L1A$), 37.002 sec; and Rotor ($L1B$), 36.750 sec.

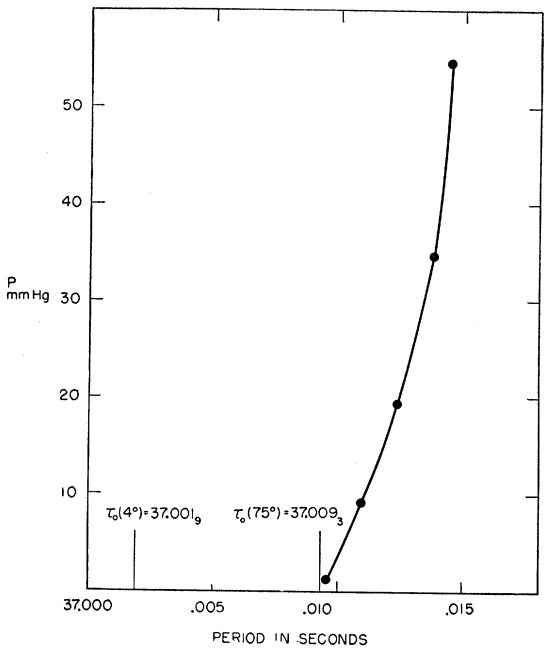

FIG. 5. Determinations of rotor period in vacuum at liquid nitrogen temperature.

[20] Altman, Rubin, and Johnston, Ohio State University (unpublished).

This indirect procedure was devised after the failure of attempts to measure the vacuum periods of Rotors ($L1A$) and ($L1B$) at liquid helium temperature. These attempts consisted of period measurements after the bath level had fallen below the bottom of the rotor, which then oscillated above the liquid in cold helium gas at low pressure.[21] Periods under these conditions indicated that some liquid remained between the plates for several hours after losing contact with the bath, for the periods were higher than had been measured at 75°K, and decreased slowly with time. The periods tended to reach the 75°K value approximately, but soon after began to increase, indicating that the now dry rotor was warming.

In the case of Rotor ($L2$), improved radiation shielding and prolonged observation gave a successful direct measurement of τ_0 at liquid helium temperature. After contact between the rotor and bath was broken, drops of liquid fell from the rotor for two to three hours, while the period generally decreased. The period eventually reached a minimum of 40.041 sec and remained at this value for over 12 hours more. The bath vapor pressure at this time was less than 0.05 mm Hg. The period of Rotor ($L2$) at 75°K was measured to be 11 milliseconds greater, whereas the increase computed from the expansion coefficient is only 8 milliseconds. The uncertainties in the τ_0 (4°K) of Rotors ($L1A$) and ($L1B$) are therefore estimated at 3 milliseconds. The measured value $\tau_0=40.041$ sec for ($L2$) has an estimated uncertainty of 1 millisecond.

The vacuum decrements of both rotors were less than 2×10^{-4}.

The vacuum decrement of Disk (L) was obtained by pumping the empty cryostat over night and then filling the outer Dewar with liquid nitrogen in order to trap out the residual air (the annular space of the He Dewar was in this case charged with He gas to a few mm pressure); Dewar space vacuum was $\sim10^{-6}$ mm Hg. The resulting vacuum decrement was $\delta_0=4.13\times10^{-4}$. The Disk ($L$) vacuum period $\tau_0=6.298$ sec at liquid helium temperatures was the average of 175 oscillations while the liquid He bath, at a level ~3 cm below the disk, was maintained at 0.22-mm pressure.

IV. EXPERIMENTAL RESULTS

Measurements in Liquid Helium

Single Disk

At the beginning of each liquid helium run, the cryostat was filled to a level of approximately 50-cm depth above the disk. Upon pumping the liquid to below the lambda point, the liquid level was reduced to approximately 30 cm. Temperatures at which the liquid was to be studied were achieved by setting the bridge circuit of the electronic bath regulator for the appropriate carbon thermometer resistance and then throttling pumping valves until the regulator controlled at approximately 10^{-3} watt input to the bath heater. An equilibration time of approximately 5 minutes was usually required for each new temperature setting after which there was no significant change in the vapor pressure of the bath.

After checking the rest position of the light beam, the pendulum was set into oscillation at an initial amplitude of 0.1–0.5 radian. Successive amplitudes during the decay of oscillations were recorded directly on semilogarithmic graph paper. We verified the original observation of Hallett[7] that an unusual dissipative mechanism appears at sufficiently high amplitudes. This paper is concerned solely with the subcritical velocity region; consequently, our interest was limited to the low-amplitude range of constant logarithmic decrement. In this range we observed at least 30 successive swings, until the amplitudes decreased by a factor of 3–5. The logarithmic decrement was determined from the slope of the best visual fit of straight line through the data. At least two complete decay curves, from the "critical amplitude" down to about 0.02 radian, were observed at each temperature; the disagreement between the decrements of the individual decay curves for each temperature was not greater than 1 percent. We obtained the Disk (L) period τ at each temperature from the average of at least two sets of ten oscillations each. The averages of each set were in agreement to within 2 milliseconds. During each experimental day, decrements were obtained in a pattern so as to provide at least two transits of the accessible temperature range, a procedure which demonstrated that there was no perceptible effect due to variations in bath height. Succeeding runs were carried out at temperatures between points previously obtained. No systematic displacements could be perceived.

Experimental values of δ for Disk (L) are tabulated in Table II and shown graphically in Fig. 6.

Finned Rotors

Measurements were carried out with Rotors ($L1$) and ($L2$) according to a procedure similar to that employed during the Disk (L) studies. In this case, however, the most important information was the period of oscillations. At least three sets of ten oscillations each yielded an average period at each temperature; mean deviations in the average period were within 3 milliseconds, giving an uncertainty within 8 parts in 10^5. Occasional observations of the logarithmic decrement were obtained in order to insure that period measurements were conducted over the subcritical amplitude region. In cases where a semilog plot was not made, decrements were obtained from the initial and final amplitude readings taken during the period measurements.

The periods showed no significant trend with am-

[21] E. L. Andronikashvili (private communication). This procedure was similar to that carried out by Andronikashvili.

TABLE II. Decrements of single Disk (L).

T °K	$10^3\delta$	T °K	$10^3\delta$
2.1236	8.56±0.03	1.287	2.53±0.01
2.0433	6.84±0.02	1.392	2.72±0.02
1.306	2.50±0.01	1.594	3.47±0.01
1.461	2.97±0.03	1.7978	4.42±0.02
1.8898	5.22±0.04	1.9311	5.50±0.01
2.1658	9.98±0.07	2.0042	6.28±0.03
1.682	3.53±0.03	2.1442	9.12±0.00
2.1691	10.17±0.06	2.1727	10.41±0.06
2.1579	9.60±0.03	2.1669	10.13±0.05
2.0931	7.70±0.03	2.1409	8.94±0.06
1.8572	4.88±0.01	1.063	1.96
1.689	3.90±0.02		
1.492	3.00±0.01	δ_0	0.413
1.320	2.39±0.03		

plitude in the subcritical region. The rest position of the optical lever shifted by <0.001 radian over the accessible temperature range; this shift was possibly due to a distortion of the torsion head due to the change in pressure. There was no perceptible change of period with bath height.

Calculation Scheme

The equations of motion of the oscillating bodies are obtained from the individual moments of inertia and dimensions corrected for thermal contraction, the periods and decrements, and the pertinent equations derived in Sec. II of this paper. Estimated effect of liquid and vapor damping on the stiff rod showed that this contribution to the nuisance damping was insignificant in our case; we accordingly use the vacuum decrement. We also employ the experimental corner parameter $\bar{\nu}=0.34$.

The Disk (L) formula, after Eq. (27) is thus

$$\rho\eta=\frac{0.06089}{\tau(1-\delta)}\left\{\frac{\delta[(\tau/\tau_0)^2+1]-1.302\times10^{-4}\tau}{1+1.269\lambda}\right\}^2. \quad (32)$$

Penetration depths encountered in the Rotor ($L1$) studies were 2–8 times the spacing between the disks; the assumption that the peripheral boundary is a smooth cylinder in a hydrodynamic sense appears to be justified. Therefore, the formula applicable to the motion of the finned rotors is Eq. (30b). However, the simpler Eq. (31) may be used when the slippage of liquid contained between plates is negligible. A preliminary estimate of the "fraction of slip," defined as $1-F_2(2s/\lambda)^{-1}$, gave a maximum figure of about 0.1% in a gap equal to the mean disk spacing. A direct check of the estimate is afforded by the damping Eq. (30a). It can be seen that in the case of zero slip, the rotor behaves like a single disk of thickness equal to the total height of the stack. This condition is approached only asymptotically. Although the fraction of slip may be reduced to a small value for the purpose of determining the liquid density from period measurements, the "internal friction" due to the residual slip is enhanced

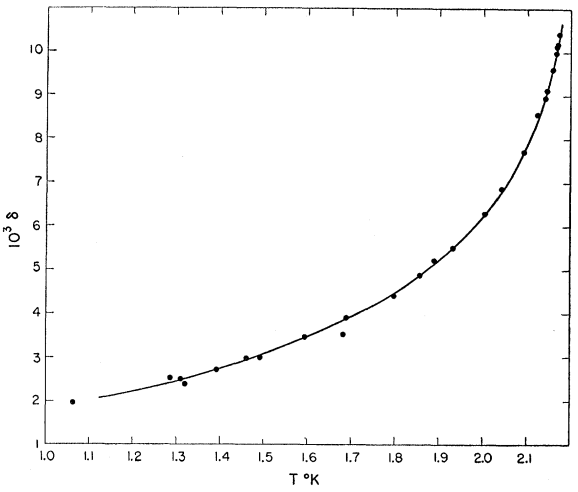

FIG. 6. Decrements of Disk (L) in He II.

by the large surface area of the many disk faces over which the drag acts, causing a large contribution to the decrement. This magnification of the effect upon the experimental decrement prevents one from obtaining reliable $\rho\eta$ measurements with a finned rotor from Eq. (30a). Equation (30a) and the observed decrement may be safely employed, however, to obtain an experimental measurement of slippage by solving for the function F_1. Thus, we employed the measured excess of damping of Rotor ($L1A$) above that of a solid disk in the neighborhood of the lambda point to obtain an experimental value for the "internal damping factor" F_1 of Eq. (30a). The experimental value of F_1 corresponds to a slippage of 0.113% at T_λ, in agreement with the value estimated directly from the average disk spacing and the penetration depth. Since the penetration depth increases monotonically from the lambda point to lower temperatures, the liquid between the disks is set into motion with an efficiency no lower than 99.89%, and we may use Eq. (31) with corresponding accuracy in the computed liquid density.

The equations pertinent to the Rotor ($L1$) are

$$\text{Rotor } (L1A): \quad \rho=\frac{0.60428[(\tau^*/\tau_0^*)^2-1]}{1+1.50\lambda^*+0.57\lambda^{*2}}, \quad (33a)$$

$$\text{Rotor } (L1B): \quad \rho=\frac{0.60254[(\tau^*/\tau_0^*)^2-1]}{1+1.50\lambda^*+0.57\lambda^{*2}}. \quad (33b)$$

The equation applied to Rotor ($L2$) was, after Eq. (30b),

$$(\rho\eta\tau^*)^{\frac{1}{2}}=\frac{0.11468[(\tau^*/\tau_0^*)^2-1]}{F_2+0.1375+0.0576\lambda^*}, \quad (33c)$$

with $2s=0.0805$ cm. The periods and penetration depths belonging to the rotors are starred in order to avoid confusion with the corresponding characteristics of the single disk.

TABLE III. Experimental values of density ρ_n and viscosity η in liquid He II, together with values of τ^*, τ, and δ from which they were computed.

T °K	τ^* sec	$10^3\,\delta^*$	τ sec	$10^3\,\delta$	η micropoise	ρ_n g/cm³
	Rotor ($L1A$)		Single Disk (L)			
2.1467	40.940	9.62	6.381	9.160	23.02	0.12538
2.0942	40.346	8.31	6.371	7.740	19.25	0.10496
2.1326	40.755	9.28	6.378	8.705	21.78	0.11900
2.1680	41.299	10.42	6.386	10.140	25.94	0.13772
2.0189	39.734	7.00	6.363	6.465	16.34	0.08403
1.9610	39.355	6.16	6.359	5.800	15.26	0.07108
1.8960	38.992	5.35	6.355	5.190	14.46	0.05878
1.7979	38.548	4.43	6.350	4.460	13.82	0.04387
1.701	38.195	3.84	6.346	3.940	14.23	0.03206
1.601	37.913	3.47	6.344	3.500	15.20	0.02275
2.0692	40.122	8.05	6.368	7.270	18.17	0.09727
2.1187	40.591	8.60	6.375	8.325	20.81	0.11335
2.1725	41.457	10.62	6.387	10.395	26.26	0.14339
2.1720	41.425	10.87	6.387	10.365	26.31	0.14221
2.1710	41.381	10.61	6.387	10.305	26.28	0.14063
2.1699	41.342	10.49	6.387	10.250	26.25	0.13922
2.1638	41.205	10.20	6.385	9.850	25.00	0.13458
2.1075	40.472	8.65	6.373	8.025	19.96	0.10928
2.1528	41.025	9.65	6.382	9.400	23.76	0.12827
2.0467	39.935	7.33	6.366	6.880	17.28	0.09087
1.9931	39.551	6.65	6.362	6.145	15.82	0.07776
1.9359	39.205	5.6	6.357	5.540	14.88	0.06599
1.8461	38.750	4.79	6.352	4.795	14.08	0.05063
1.7501	38.356	4.10	6.348	4.185	14.01	0.03743
1.649	38.030	3.46	6.345	3.700	14.82	0.02659
2.1581	41.114	9.78	6.383	9.590	24.19	0.13139
2.1717	41.446	11.	6.387	10.350	26.09	0.14303
	Rotor ($L1B$)					
2.0473	39.689	7.95	6.367	6.890	17.22	0.09153
2.0025	39.358	7.4	6.363	6.250	15.93	0.08018
1.652	37.789	3.9	6.345	3.715	14.67	0.02710
1.502	37.428	4.1	6.341	3.095		0.01524
1.400	37.253	4.3	6.339	2.740		0.00959
1.9365	38.967	7.0	6.357	5.550	14.75	0.06683
1.140	37.000		6.335	2.105		0.00159
1.132	36.988		6.335	2.085		0.00121
2.0499	39.708	8.1	6.367	6.935	17.33	0.09218
1.287	37.113	4.6	6.337	2.425		0.00512
1.255	37.084	4.9	6.336	2.345		0.00421
1.221	37.050	5.4	6.336	2.275		0.00313
1.218	37.045	7.0	6.336	2.265		0.00296
1.354	37.190	4.2	6.339	2.605		0.00757
1.8505	38.530	5.3	6.352	4.825	13.91	0.05199
1.452	37.334	4.0	6.340	2.915		0.01220
1.598	37.645	3.5	6.344	3.480		0.02235
1.651	37.791	4.2	6.345	3.710	14.59	0.02719
1.7473	38.094	6.1	6.348	4.170	13.95	0.03729
1.8974	38.756		6.355	5.205	14.35	0.05964
2.1724	41.219	10.8	6.387	10.380	25.96	0.14466
1.8002	38.315	4.7	6.350	4.475	13.64	0.04476
1.6975	37.943	4.4	6.346	3.925	14.03	0.03226
1.553	37.543	3.1	6.342	3.295		0.01901
1.327	37.156		6.337	2.525		0.00649
	Rotor ($L2$)					
1.597	40.674	5.01	6.344	3.480	15.07	0.02231
1.500	40.498	3.27	6.341	3.080	16.18	0.01536
1.406	40.359	2.54	6.339	2.760	18.50	0.01004
1.309	40.250	2.26	6.337	2.480	22.71	0.00596
1.212	40.170	1.92	6.336	2.255	31.36	0.00302
1.172	40.149	2.18	6.335	2.170	35.27	0.00229
1.700	40.903	7.25	6.346	3.930	14.06	0.03202
1.793	41.146	10.0	6.350	4.430	13.74	0.04326
1.382	40.325	2.82	6.339	2.685	19.61	0.00874
1.453	40.418	3.84	6.340	2.920	17.59	0.01225
1.549	40.580	3.86	6.342	3.280	15.67	0.01855
1.649	40.784	5.65	6.345	3.700	14.51	0.02687
1.748	41.019	8.42	6.348	4.165	13.84	0.03725
1.268	40.207	2.29	6.336	2.380	26.70	0.00435

Values of the liquid density and viscosity are obtained from the experimental τ, δ, and τ^* at each temperature, by simultaneous solution of Eq. (32) and Eq. (33). Although the same range of temperatures was studied with the disk and the rotors, the fixed temperatures in the different studies did not precisely correspond. The values of δ and τ of the disk appropriate to the temperatures studied with the rotors were therefore obtained by interpolation of the disk data. Large plots of the experimental Disk (L) data were fitted with smooth curves, from which the necessary information was obtained. Mean deviation of the data points about the smooth curve is about 1%.

ρ and η were computed at each temperature on an IBM 701 computer, using the method of successive approximations. Iterations were carried out until fractional changes in the kinematic viscosity η/ρ were less than 0.01%.

Comparison between the densities given by Rotors ($L1$) and ($L2$) at temperatures 1.2°–1.8°K showed the ($L1$) values to be larger by an amount corresponding to the systematic excitation of 3.4% of the superfluid present. This discrepancy is consistent with the observed mechanical defects of the more delicate system. We therefore applied the indicated correction to all densities and viscosities obtained from iterations of the Rotor ($L1$) data. This correction varied from zero at T_λ to almost 8% at 1.8°K, the highest temperature for which ($L2$) data is given.

Experimental values of the density and viscosity are given in Table III, together with τ^*, τ, and δ from which they were computed.

Discussion of Errors

Dimensions of Disk (L) were measured at room temperature with calibrated micrometers, to an accuracy of about 5×10^{-4} cm. Density of the disk material was measured to 0.1%. The calculated disk coefficient $4I^2/\pi a^8$ is thus known to approximately 2%. The moment of inertia of Rotor ($L1$), measured by the comparison method described in Sec. III, is accurate to 0.3%. Uncertainties in the measured dimensions of the rotor, together with the discrepancy in the moment, lead to a possible error in ρ_n of 0.5%. Corrections due to thermal contraction amount to about 1.6% in $\rho_n\eta$ and 0.8% in ρ_n; these corrections are determined to an accuracy of better than 5%.

Reproducibility of the measured decrements of Disk (L) was in general better than 1%; corresponding uncertainty in $\rho_n\eta$ is 2% at the lambda point and up to 4% at 1.2°K. Uncertainties in the periods of Disk (L) cause negligible errors.

As discussed in Sec. III, errors in the technique of rotor period measurement amount to no more than 5 milliseconds. Periods in He II were reproducible to 5 milliseconds. The uncertainty in ρ_n due to the above timing errors is 3×10^{-4} g/cm³ at all temperatures.

The corner parameter is the principal source of error in the hydrodynamic equations. Experimental scatter in ν causes an uncertainty in Disk (L) $\rho_n\eta$ values of 0.3% near the lamdba point and 1.5% at the lowest temperatures. Corresponding uncertainty in ρ_n is within 0.2%. Neglect of squared and higher order terms in λ introduce errors no greater than 0.3%. Slippage of the viscous fluid between the rotor plates of ($L1$) never exceeds 0.1%, in agreement with the theoretical estimate. Slippage was accounted for in the equation applied to Rotor ($L2$).

Errors in the machine computations of ρ_n and η are insignificant.

Hence, the total nonsystematic error in ρ_n is 1% at high temperatures and 6% at 1.2°K. Maximum random eror in η is 5% at the lambda point and 9% at low temperatures.

V. DISCUSSION

Normal Fluid Density

The behavior of ρ_n in the neighborhood of the lambda point has been investigated in detail. Data for this region are given graphically in Fig. 7. Several experimental points taken within 5 millidegrees of T_λ show a satisfactory approach to the pycnometer value[22] of ρ_λ at 2.1735°K, the transition temperature determined earlier in a different apparatus.[23] A particularly interesting feature of Fig. 7 is the sharp upturn within 0.01°K of T_λ; we found, in fact, that in this region the rotor period was a more sensitive indicator of temperature variations than the manometer levels.

The unusual behavior of the density near the lambda point can be seen also in the nature of the temperature derivative $\rho_n^{-1}d\rho_n/dT$. This coefficient has a form resembling an ordinary thermal expansion coefficient $\alpha=-\rho^{-1}d\rho/dT$; ignoring the difference in sign, we define $\alpha_n=\rho_n^{-1}d\rho_n/dT$ as the "thermal coefficient of the normal fluid." Its experimental behavior, obtained from tangents drawn to large smooth curves through the data, is shown in Fig. 8. The coefficient is closely proportional to $1/T$ from 1.2° to 2.0°K; deviation from the inverse temperature dependence begins at about 2.0°K. The marked rise in α_n as T_λ is approached is most striking; it increases by a factor of two for a change of 1 millidegree at 2.1725°K. Although it was not possible to measure α_n exactly at T_λ, the behavior at lower temperatures suggests that $\alpha_n(T_\lambda)$ is infinite. Recent measurements by Atkins[24] indicate that the expansion coefficient $-\alpha$ of the whole liquid tends to infinity at the lambda point. It has a shape similar to α_n in the neighborhood of the transition, but magnitudes no greater than 0.5% of α_n at all temperatures measured below T_λ.

The inverse temperature dependence of α_n below

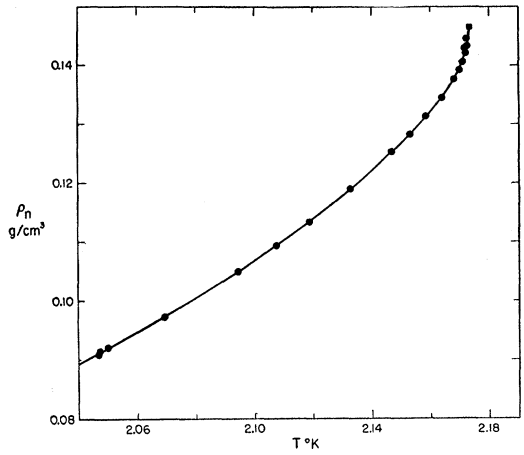

FIG. 7. Normal fluid density in the region of the lambda point. ● Rotor ($L1$); ■ total density at T_λ (reference 22).

2.0°K corresponds to the theoretical behavior predicted by Landau[25] and by Feynman.[26] According to Landau, the temperature function of the roton contribution to the normal fluid density is

$$\rho_n/\rho=AT^{-\frac{1}{2}}e^{-\Delta/kT},\quad A=\text{constant},\qquad(34)$$

where Δ/k represents the minimum energy required to excite a roton. At all temperatures investigated here,

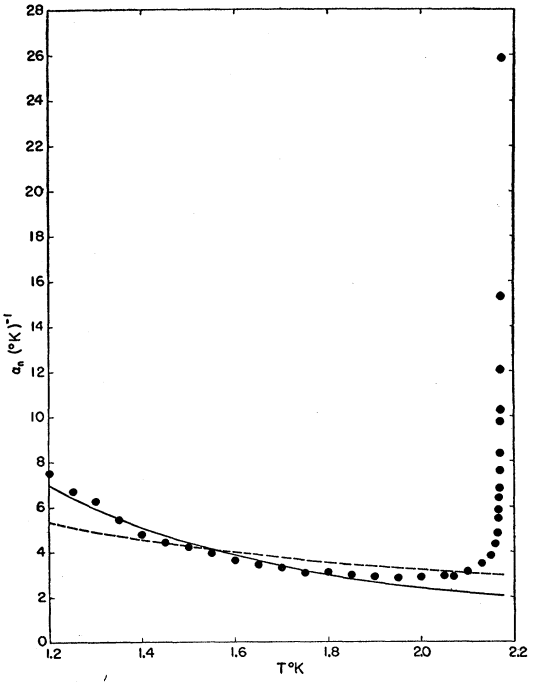

FIG. 8. Thermal coefficient of normal fluid, $\rho_n^{-1}d\rho_n/dT$. ● Experimental; —— derived from roton contribution, $\Delta/k=10.60$°K; – – – derived from power law $(T/T_\lambda)^{6.38}$.

[22] E. C. Kerr (to be published).
[23] J. G. Dash and R. Dean Taylor, Phys. Rev. **99**, 598 (1955).
[24] K. R. Atkins and M. H. Edwards, Phys. Rev. **97**, 1429 (1955).
[25] L. Landau, J. Phys. (U.S.S.R.) **5**, 72 (1941); **8**, 1 (1944); **11**, 91 (1947).
[26] R. P. Feynman, Phys. Rev. **91**, 1291, 1301 (1953).

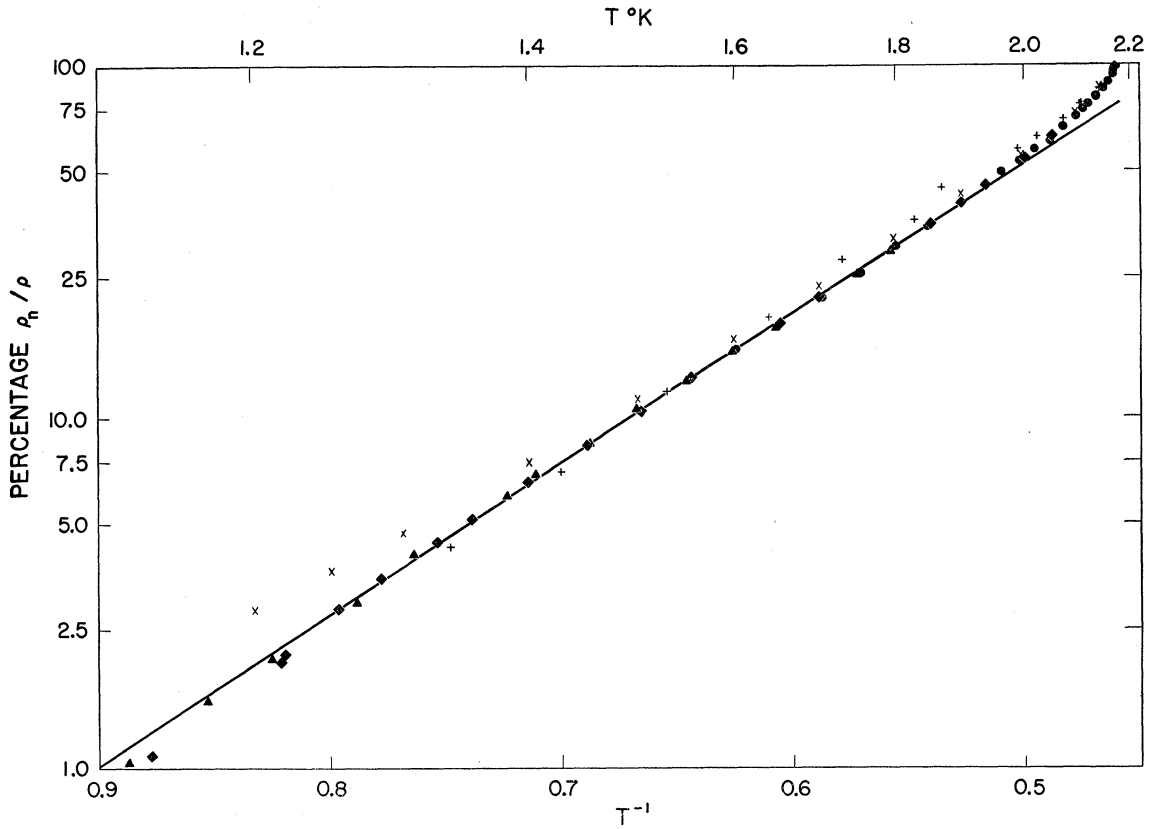

FIG. 9. Percentage of normal fluid from 1.15°K to the lambda point. ● Rotor (*L1A*); ♦ Rotor (*L1B*); ▲ Rotor (*L2*); + Andronikashvili; × derived from second sound and heat capacity; —— roton contribution, $\Delta/k=10.60$°K.

the contribution to ρ_n due to phonons is estimated to be less than 0.2% of the measured values. The density data are directly compared with the form of Eq. (34) in Fig. 9. We neglect the 0.8% variation in the total density ρ over the temperature range by taking the ratio of ρ_n to the value of ρ at T_λ.[22] The experimental points below 2.0°K are well described by the theoretical curve corresponding to the parameters $A=1.486\times10^2$(°K)$^{\frac{1}{2}}$, $\Delta/k=10.60$°K. As expected for the region of high roton concentration, the equation provides an increasingly poorer description of the density as the lambda point is approached; furthermore, the parameters chosen to represent the colder region place the point at which $\rho_n=\rho$ at the wrong temperature, 2.313°K. The coefficient α_n calculated from the above formula is compared with the measured values in Fig. 8. Deviations of the ρ_n equation from our smoothed data are given in Fig. 10; agreement averages better than 1.5% between 1.2–2.0°K, and the maximum discrepancy is 3.4% at 2.0°K. Feynman and Cohen[27] have recently recalculated Δ/k from atomic and x-ray data as 11.5°K. Normalization to our data at 1.5° yields the coefficient $A=2.75\times10^2$. The resulting values of ρ_n/ρ are approximately 14% above our data at 2.0° and 11% below at 1.2°K, in good agreement for a Δ/k value calculated from first principles.

In contrast to the correspondence obtained with Eq. (34), the alternative semitheoretical formula[28]

$$\rho_n/\rho=(T/T_\lambda)^r, \quad r=\text{constant}, \tag{35}$$

provides a much poorer description. A rough approximation to the data over the entire range is given by $r=6.38$; its logarithmic derivative is compared with α_n in Fig. 8. Deviations of this equation from the data are shown in Fig. 10; the average discrepancy below 2.0° is 5.5% and reaches 16% at 1.2°K. Only slightly better agreement is obtained when Eq. (35) is treated as a two-constant equation by choosing a better parameter for T_λ than the actual value.[29]

Normal fluid density measurements by other investigators are also included in Fig. 9. The first such study was made by Andronikashvili,[3,4] using the same experimental approach reported here. Methods of period measurement and calculation were cruder in this

[27] R. P. Feynman and M. Cohen, Phys. Rev. **102**, 1189 (1956).

[28] F. London, *Superfluids* (John Wiley and Sons, Inc., New York, 1954), Vol. II.

[29] A two-constant equation of this form was given in our preliminary report at the Louisiana State University conference. Normal density values corresponding to this equation were based upon results obtained with Rotor (*L1*) only and were therefore considerably in error at the lowest temperatures.

TABLE IV. Smoothed data at regular temperature intervals.

T °K	ρ_n/ρ %	α_n (°K)$^{-1}$	$\eta\,\mu P$	T °K	ρ_n/ρ %	α_n (°K)$^{-1}$	$\eta\,\mu P$
2.1735	100.00			2.000	54.20	2.89	15.96
2.1730	98.86	25.8		1.950	46.97	2.84	15.00
2.1720	97.22	12.1		1.900	40.68	2.89	14.39
2.171	96.12	9.75		1.850	35.13	2.98	14.04
2.170	95.28	7.56	26.1	1.800	30.07	3.10	13.88
2.169	94.54	6.80		1.750	25.60	3.09	13.92
2.168	93.93	6.38		1.700	21.85	3.30	14.14
2.167	93.36	5.84		1.650	18.35	3.44	14.51
2.166	92.83	5.47		1.600	15.40	3.63	15.01
2.165	92.30	4.80	25.2	1.550	12.70	3.95	15.64
				1.500	10.31	4.23	16.46
2.160	90.13	4.35	24.49	1.450	8.28	4.42	17.5
2.150	86.55	3.83	23.31	1.400	6.56	4.78	18.9
2.140	83.37	3.67	22.34	1.350	5.09	5.42	21.0
2.130	80.38	3.49	21.51	1.300	3.83	6.25	23.9
2.120	77.67	3.29	20.78	1.250	2.78	6.69	28
2.110	75.20	3.23	20.14	1.200	1.95	7.49	33
2.100	72.82	3.10	19.56				
2.090	70.59	3.03	19.04				
2.080	68.51	2.93	18.57				
2.070	66.56	2.91	18.14				
2.060	64.65	2.91	17.75				
2.050	62.77	2.92	17.38				

pioneer work, and are evidenced by the larger scatter of Andronikashvili's data. Within these random variations, however, we are in agreement over the entire range common to both studies. Indirect determination of ρ_n/ρ may be obtained from the heat capacity C, the entropy S, and second sound velocity U_{II}, through the use of the theoretical relation[28]

$$\rho_n/\rho=\left[\frac{C}{T}\left(\frac{U_{II}}{S}\right)^2+1\right]^{-1}. \tag{36}$$

Noting that some 10% discrepancy exists between independent measurements of the heat capacity,[30,31] we have included in Fig. 9 the ρ_n concentrations calculated from thermal[30] and second sound velocity[32] data. These calculated concentrations lie systematically higher than the torsion pendulum values at all temperatures and deviate increasingly at lower temperatures. Disagreement at 1.2°K is 45%, approximately 3 times the combined uncertainty of the different experiments. Previous authors have observed that Δ/k determinations given directly by specific heat data and by the second sound data with Eq. (36) are not consistent[31]; these data yield Δ/k varying in magnitude from about 8 to 9.6°K.

In Table IV we have listed smoothed values of normal fluid concentration and thermal coefficient at several temperatures.

[30] Kramers, Wasscher, and Gorter, Physica **18**, 329 (1952).
[31] G. R. Hercus and J. Wilks, Phil. Mag. **45**, 1163 (1954).
[32] V. Peshkov, J. Phys. (U.S.S.R.) **10**, 389 (1946); Lane, Fairbank, and Fairbank, Phys. Rev. **71**, 600 (1947); J. R. Pellam, Phys. Rev. **75**, 1183 (1949); R. D. Maurer and M. A. Herlin, Phys. Rev. **76**, 948 (1949).

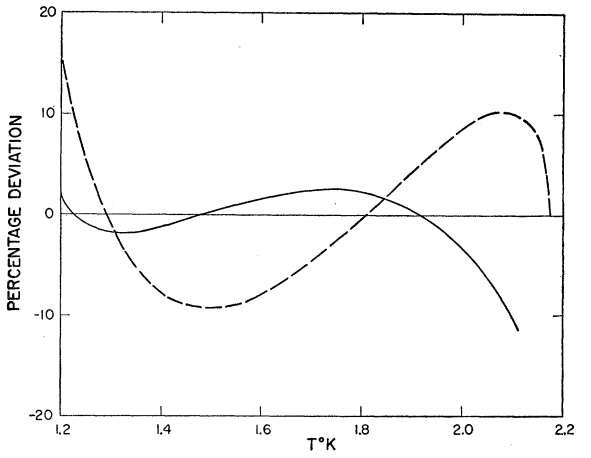

FIG. 10. Deviations of theoretical normal fluid density behavior from experimental data. —— roton contribution, $\Delta/k=10.60$°K; - - - $(T/T_\lambda)^{6.38}$.

Viscosity

The behavior of the viscosity of He II is shown in Fig. 11, in which we compare our results with those published by Andronikashvili[5] and Heikkila and Hallett.[33] Andronikashvili employed the single oscillating disk method, as in the present research. Certain approximations and the use of the "Meyer" edge correction suggest that his values should be increased by about 8%. This increase is sufficient to bring the two sets of data into agreement to within the combined experimental uncertainties. Heikkila and Hallett have recently measured the viscosity in a more direct way by means of a rotating cylinder viscometer, a method that does not require knowledge of ρ_n. Their data parallel our results between T_λ and 1.5°K, but are lower by about 9%. The effect of thermal contraction on their apparatus was neglected; the viscometer results should therefore be raised by an estimated 4%.[33] The viscometer and single-disk data are consequently in agreement between T_λ and 1.5°K. Below 1.5°, however, the viscometer results deviate systematically from the single-disk measurements; at 1.2°K, Heikkila and Hallett report 19.6 micropoise, while we find a value of about 33 micropoise. The discrepancy is much larger than can be expected from the uncertainty in our ρ_n values, especially since a mechanically imperfect rotor tends to yield ρ_n values too large, and hence erroneously decreases the calculated viscosity. The reported instability of the viscometer suggests that results obtained from it are less reliable at lower temperatures, but we cannot estimate the uncertainty of the results. Should Disk (L) be slightly warped, however, the viscosity would be unnaturally increased principally at the lowest temperatures. Through its influence on the penetration depth, errors in the viscosity cause corresponding but smaller errors in the calculated values of ρ_n. A decrease

[33] W. J. Heikkila and A. C. Hollis Hallett, Can. J. Phys. **33**, 420 (1955).

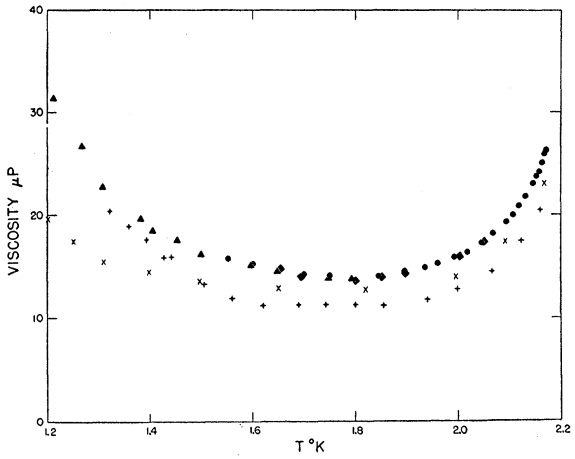

FIG. 11. Viscosity of normal fluid. ● Rotor (*L1A*); ♦ Rotor (*L1B*); ▲ Rotor (*L2*); + Andronikashvili; × Heikkila and Hallett.

in η corresponding to the discrepancy of some 50% at 1.2°K would, for instance, cause an increase in ρ_n of 12% at the same temperature. The effect on ρ_n of changes in η decreases quickly at higher temperatures; a 50% change in η at 1.3°K influences the computed ρ_n by only 7%. Although no eccentricity of Disk (*L*) was visible, we cannot rule out the possibility of some slight imperfection in its motion.

The viscosity appears to exhibit a temperature dependence similar to that of ρ_n at temperatures approaching T_λ. A more detailed study of the viscosity in He I and He II in the neighborhood of the lambda point will be published in a subsequent paper.

Smoothed values of η below 2.170°K are listed in Table IV.

VI. SUMMARY AND CONCLUSIONS

These measurements, based upon the hydrodynamic equations derived in Sec. II, have yielded data on the viscosity and density of the viscous fraction of He II. Although at no point in the experiment or calculation has it been necessary to attribute any particular qualities to the liquid other than the presence of a classical viscosity, the procedure has obviously measured the density and viscosity of the "normal fluid" only. In this respect, the analysis in no way depends upon any of the proposed theoretical models of He II.

At temperatures below 2.0°K, the quantum-mechanical liquid model of Landau and of Feynman agrees with the observed behavior of ρ_n; the experimental excitation temperature $\Delta/k=10.6°$ is closer to the calculated value of 11.5° than has been derived from thermal and second sound data. The lack of agreement between the torsion pendulum results and those calculated from less direct methods appears to be beyond the experimental uncertainties involved.

Theory has not succeeded in describing the properties of He II in the neighborhood of the lambda point; the character of the coefficient α_n near T_λ suggests that the He I—He II transition is a stronger singularity than previously supposed. In addition, the viscosity and normal fluid density are similar functions of the temperature in the highly anomalous region, indicating that these properties are equally bound to the fundamental nature of the transition. This high-temperature range of He II is apparently quite different in nature from the region below 2.0°K; the difference is shown both in the variations of α_n and in the kinematic viscosity.

ACKNOWLEDGMENTS

This research is an extension of an experimental study suggested to us by Dr. H. S. Sommers, Jr., who also assisted in the initial stages of the program. Throughout the course of this work, Dr. Louis Goldstein has given very valuable advice and criticism on the theoretical aspects of the problem, for which we are extremely grateful. We thank Mr. Max Goldstein and the computing group for carrying out the necessary iterations. The chronograph was constructed according to a design of Dr. W. L. Briscoe. Finally, we thank the members of our liquefaction and machine shop groups for their cooperation.